Satellite-based Sun-Induced Chlorophyll Fluorescence in the Greater Alpine Space: Spatial Patterns and Relationship to Gross Primary Productivity

Gomarasca, U.[1], Duveiller, G.[2], and Cescatti, A.[2], Wohlfahrt, G.[1]

[1] Department of Ecology, University of Innsbruck, Innsbruck, Austria

[2] European Commission Joint Research Centre, Ispra, Italy

Content

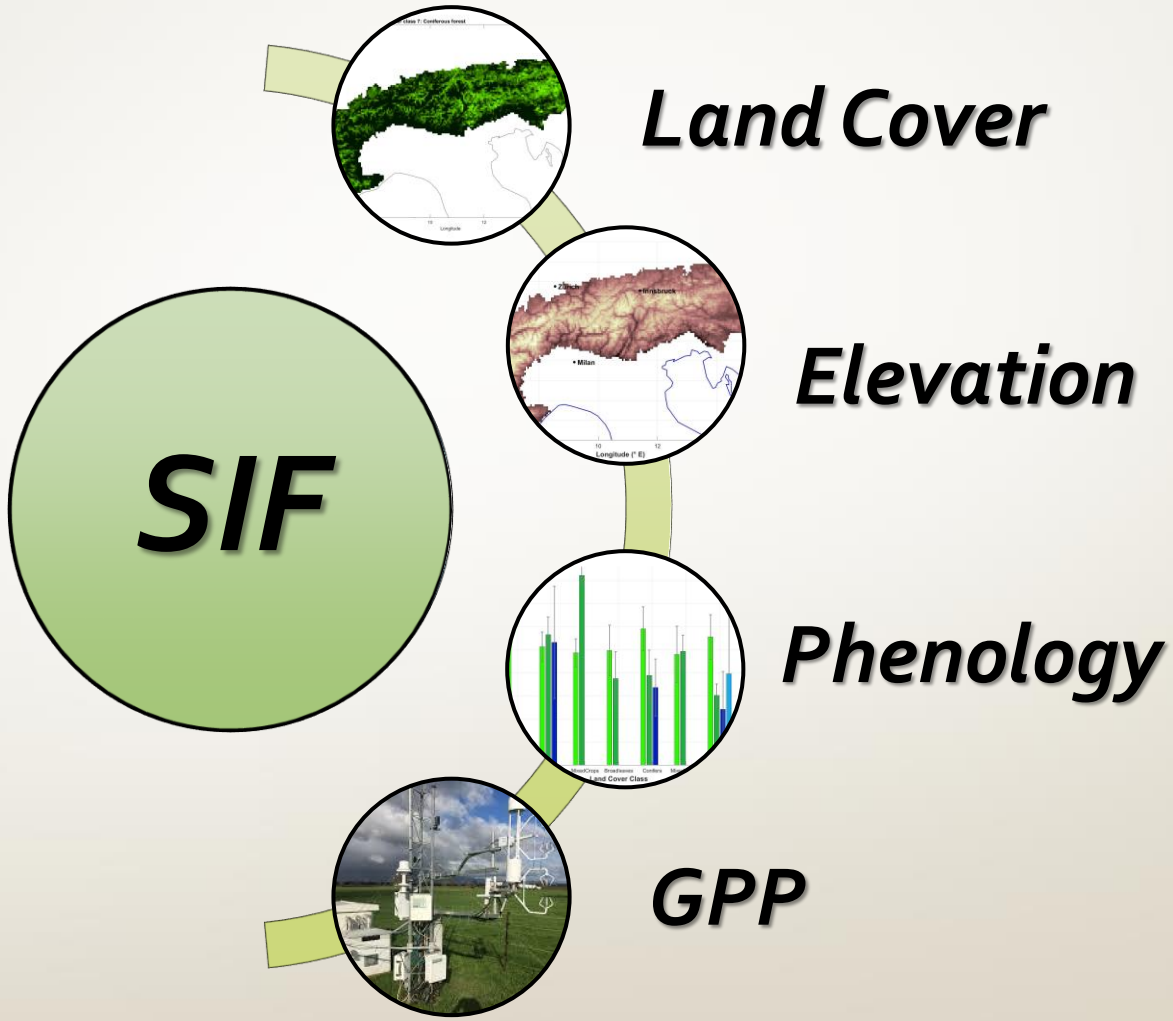

Aims

- Analyze downscaled GOME-2 SIF product over Alps:
  - Spatiotemporal SIF dynamics
  - Link environmental Land Cover and Elevation
  - Land Phenology Metrics
  - SIF-GPP relationship

Hypothesis

1. Current SIF products insufficient for heterogenous ecosystems
2. SIF-GPP relationship biome-specific at the landscape scale
3. Land cover and elevation pivotal for SIF patterns in mountainous ecosystems

SIF

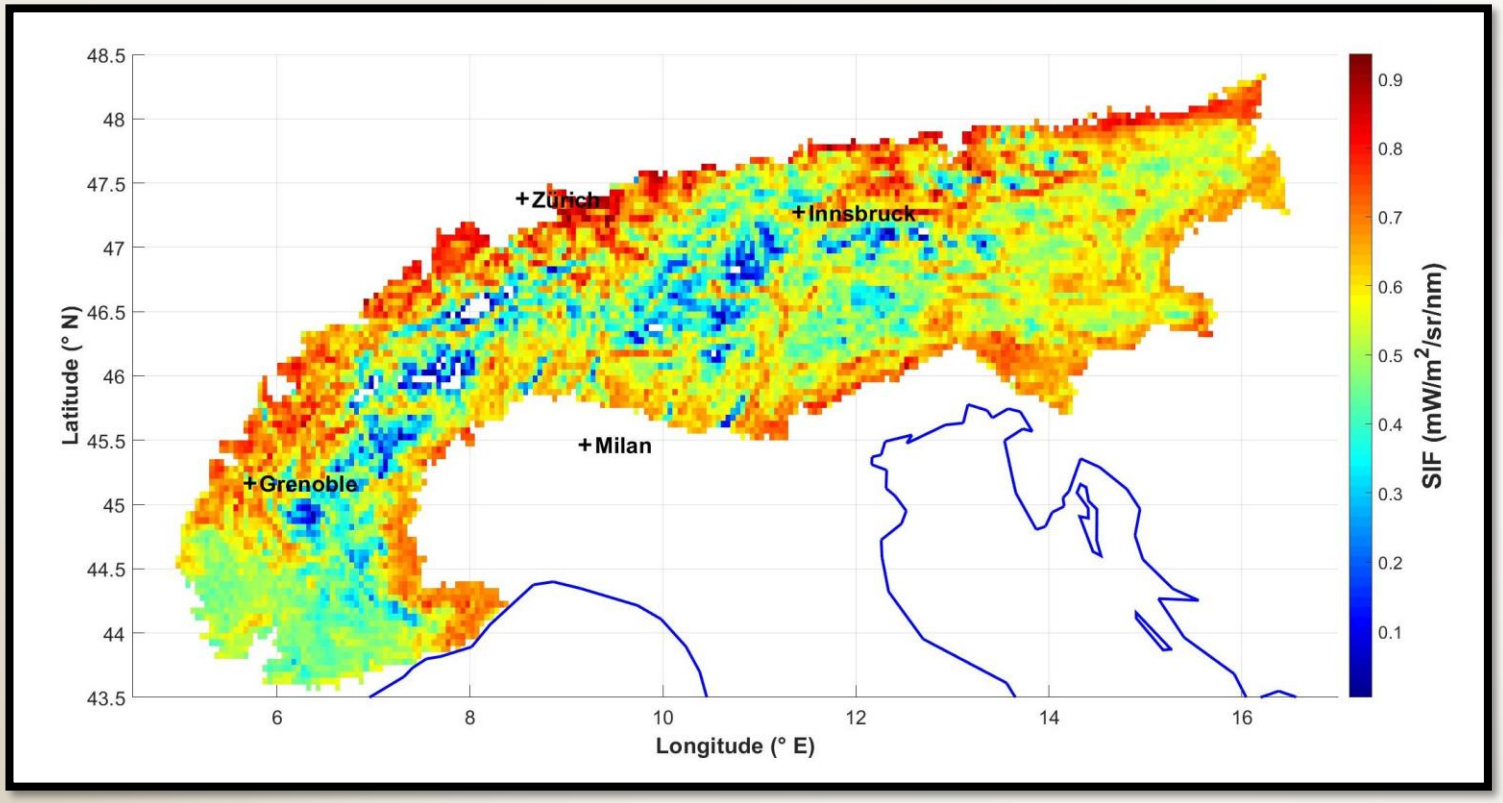

Fig. 1 – SIF over the Alps.
SIF from downscaled GOME-2 product over the study area, averaged over the entire period of data availability (2007-2017).

- Downscaled product (Duveiller et al., 2019)
- 0.05° x 0.05°, 8 d aggregation

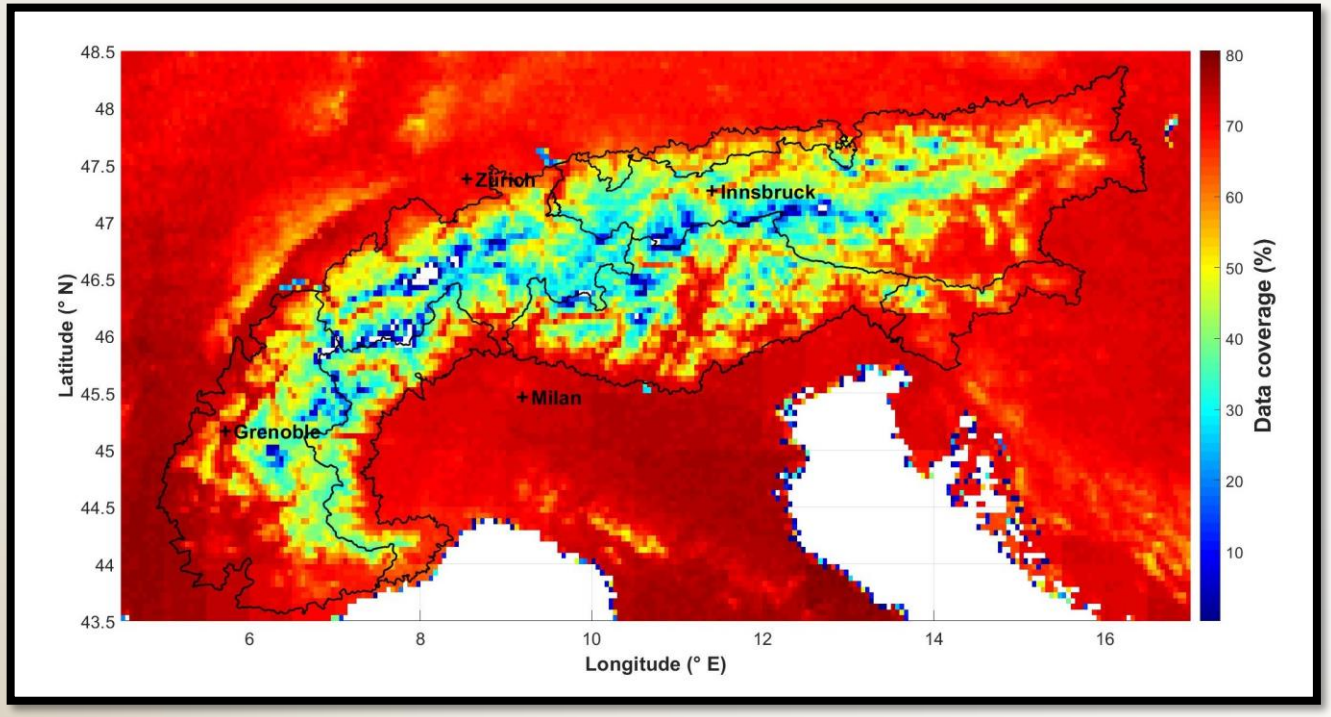

Fig. 2 – Spatial Gaps Statistics.
Percentage of data temporal coverage over the entire period (2007-2017), and Alps boundary (black outline, including state borders).

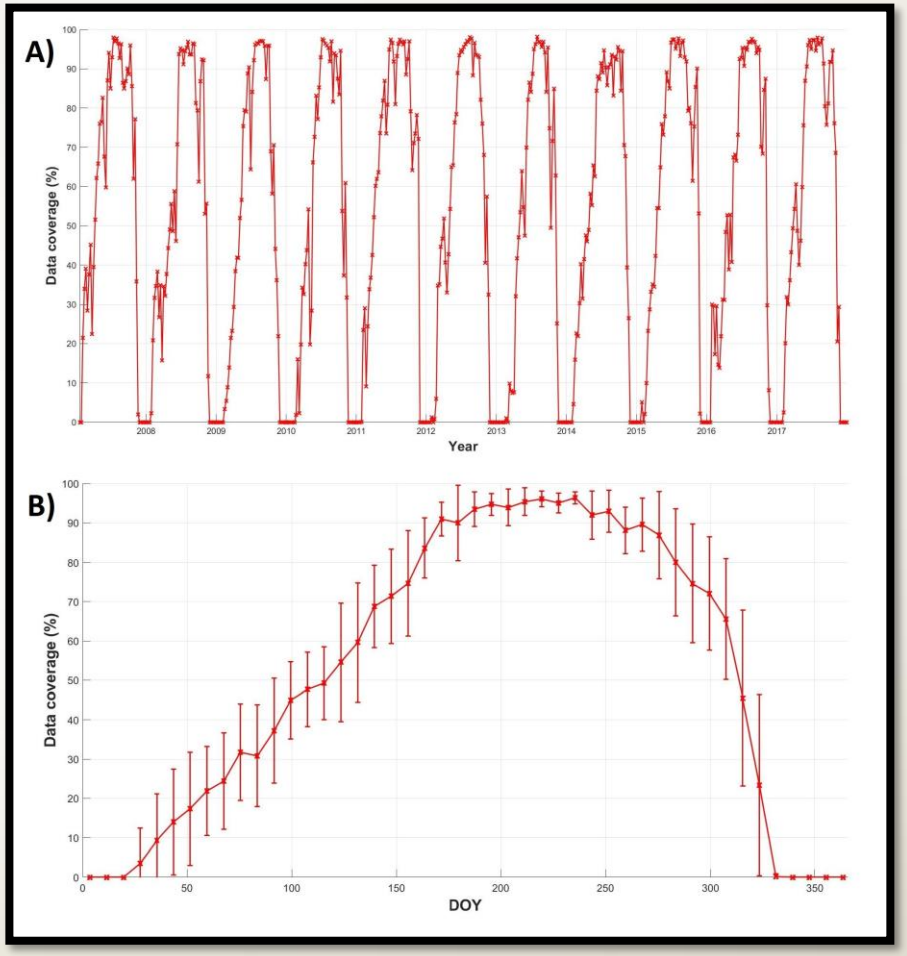

Figure 3 – Temporal Data Coverage.
GOME-2 downscaled SIF data coverage over time. A) Time period 2007-2017; year labels refer to the start of the year. B) Average data coverage (%) with standard deviation over the year for the period 2007-2017.

Gap Statistics

Land Cover Upscaling

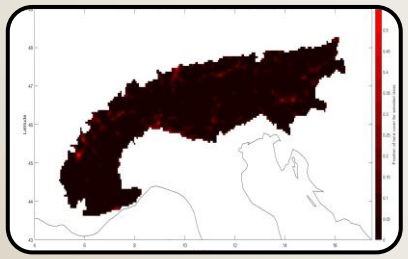

Alps mask

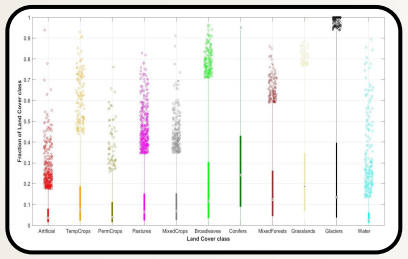

11 Land Cover Classes (LCC)

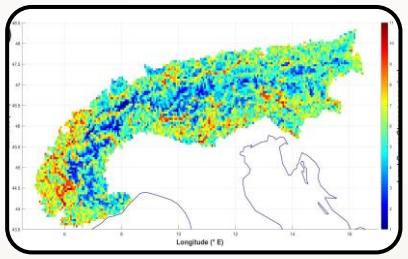

LCC fractions

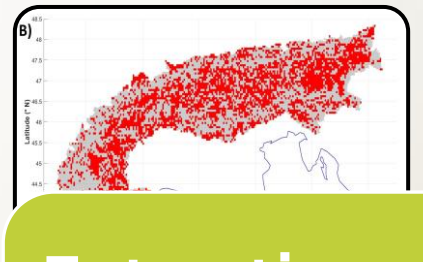

Extraction:

- Dominant-LCC (> 50 %)
- Most common combinations

Dominant LCC

Most common LCC combinations

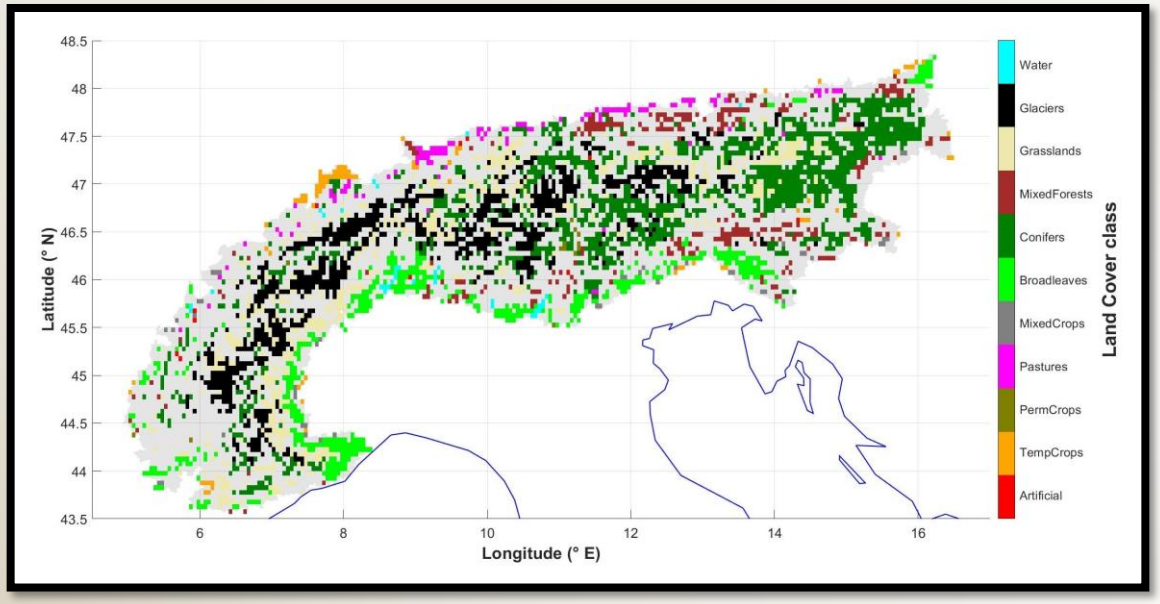

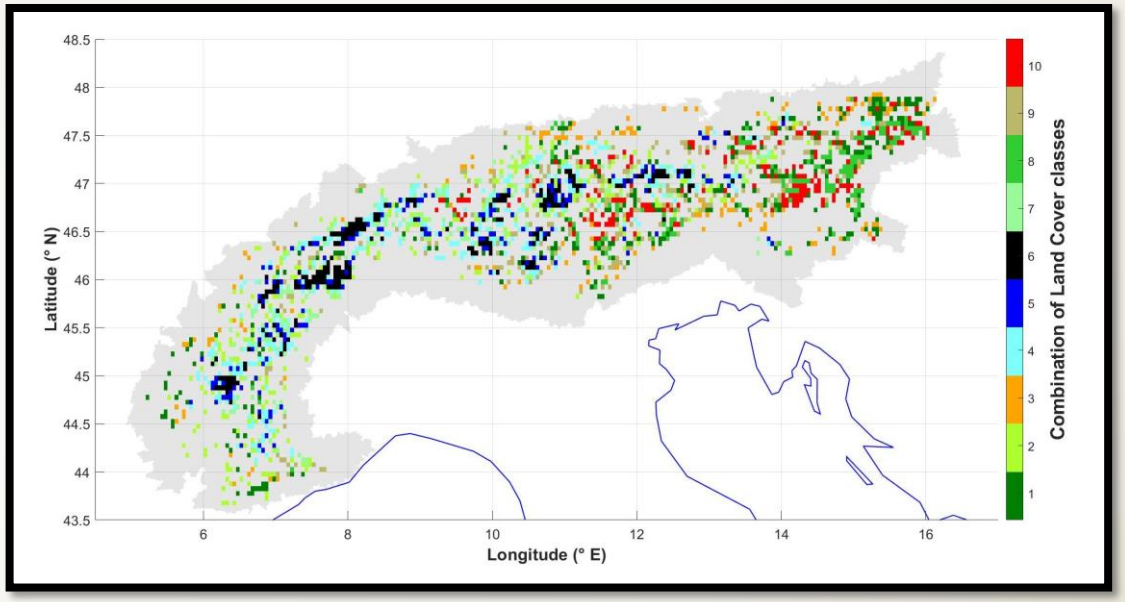

Fig. 4 – Land Cover classes extraction approaches.
Dominance of single LCC (47 % total coverage, **left**); most frequent combinations of LCC (26 % total coverage, **right**). Combinations: 1 = conifer forests (1); 2 = grassland + glacier + conifers; 3 = conifers + mixed forest; 4 = glaciers + grassland (1); 5 = mostly glaciers; 6 = 100 % glaciers; 7 = glaciers + grassland (2); 8 = conifer forests (2); 9 = conifers + grassland; 10 = conifers + pasture.

→ Further analysis with dominant-LCC extracted data

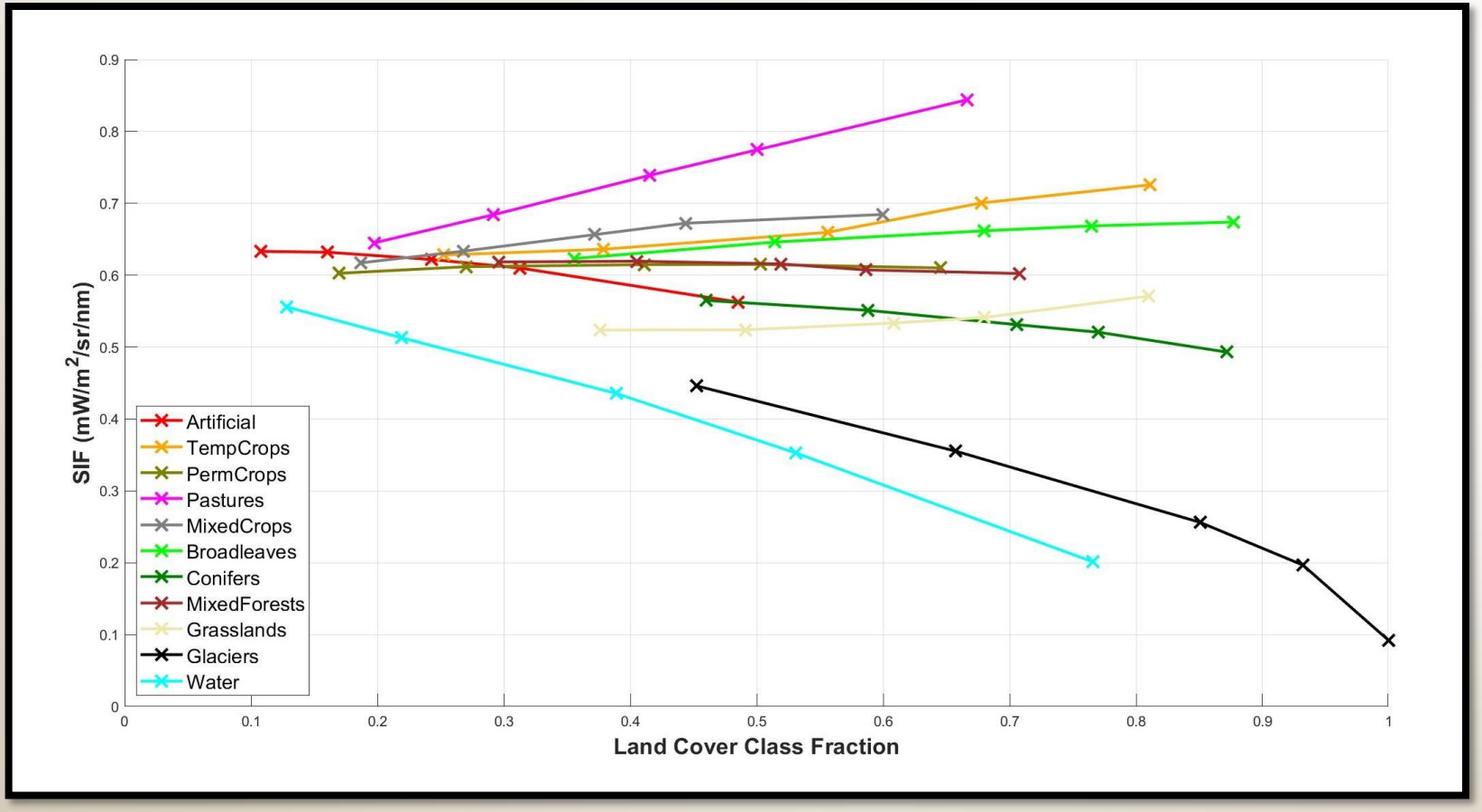

Fig. 5 – SIF for LCC at Increasing Quantiles.
SIF means at specific fraction of Land Cover classes, over quantiles for the cumulative probability of 50, 75, 90, 95, and 99 %. Error bars are not shown for clarity.

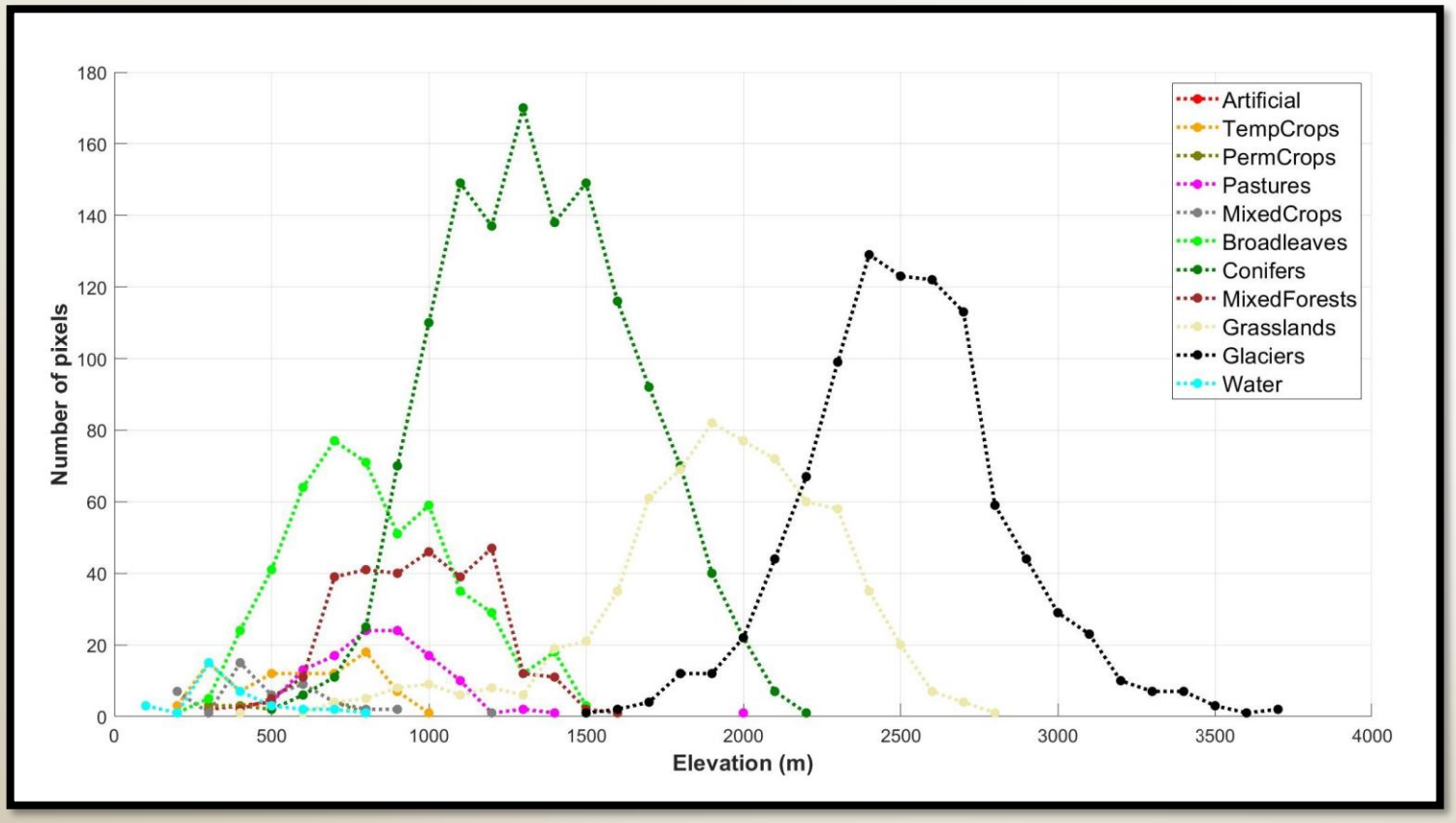

LC *vs* Elevation

Fig. 6 – Dominant-LCC vs Elevation. Number of pixels with dominant coverage for each land cover class at different elevations.

Phenology fitting algorithm

$$f(x) = a + \frac{b}{1 + \exp\left(-c(x-d)\right)} - \frac{g}{1 + \exp\left(-h(x-m)\right)}$$

Equation 1: after (Gonsamo et al., 2013)

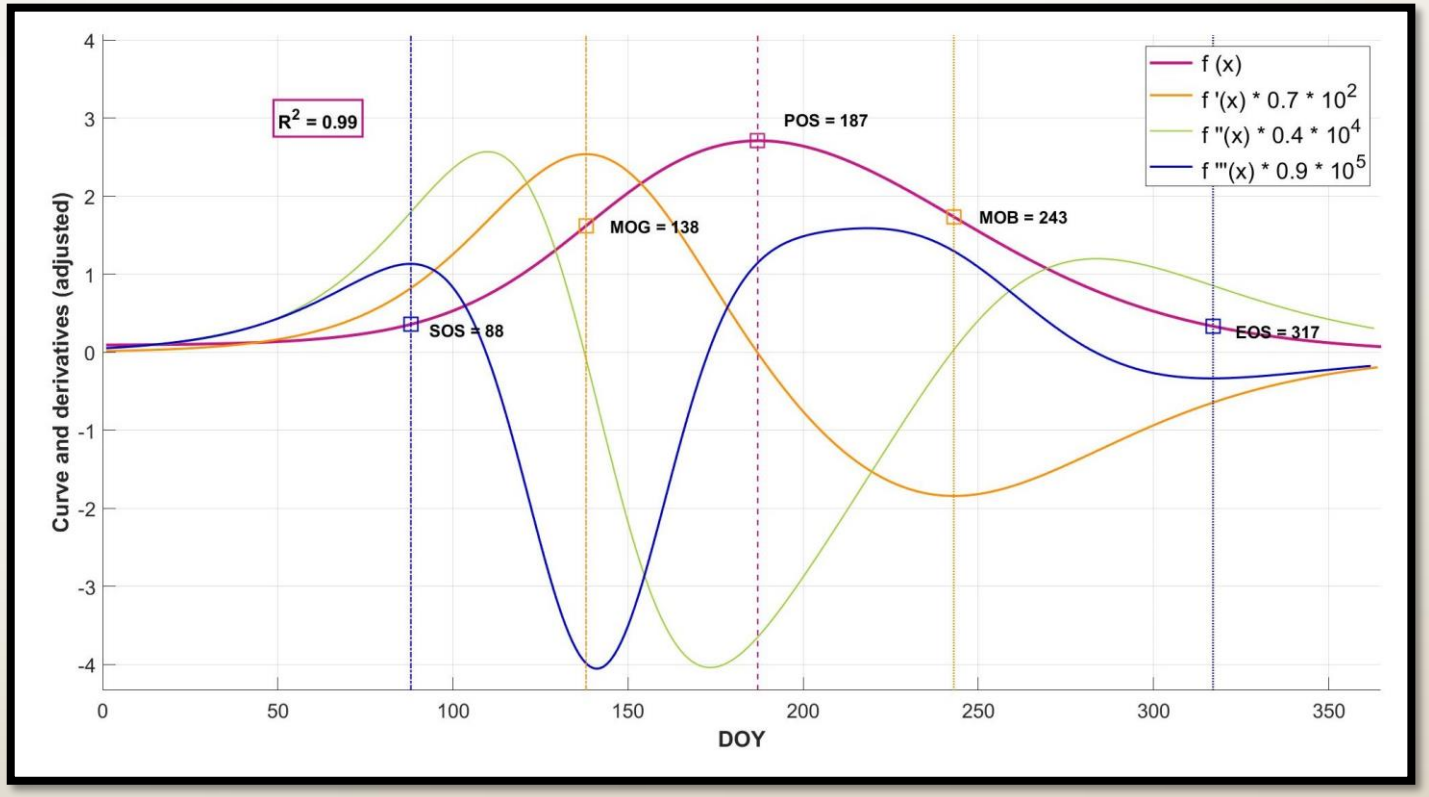

Fig. 7 – Curve Fitting for LPM.
Example of an idealized seasonal SIF-based phenological curve with derivatives, from which the appropriate phenological parameters are inferred.

Phenology

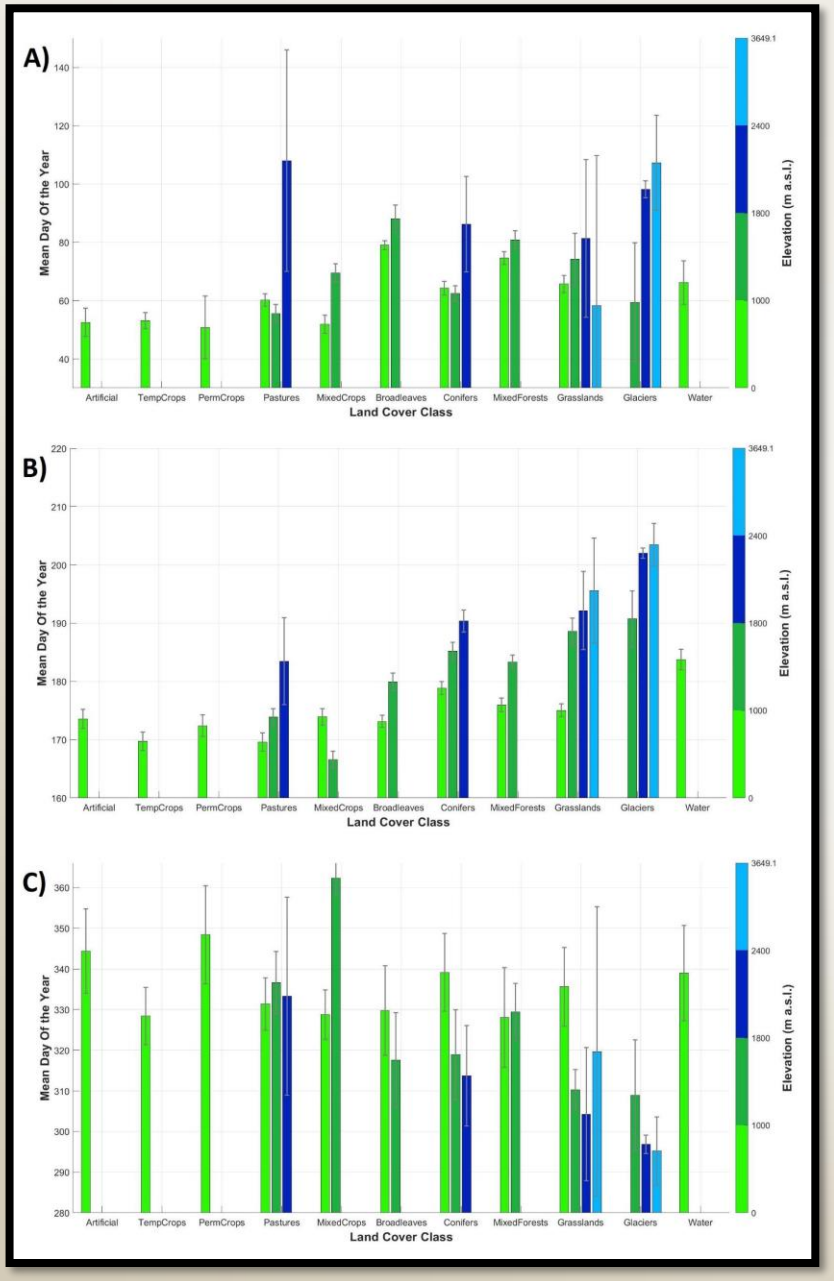

- Fit: non-linear least squares to double-sigmoidal equation
- Bootstrapping (n = 1000)
- LPM over LC classes and elevation bands

Fig. 8 – Land Phenology Metrics over LCC.
DOY of phenological indicators with standard deviation over bootstrapped data (1000 iterations) for each land cover class at each elevation band where data are present. **A)** Start Of Season (SOS); **B)** Peak Of Season (POS); **C)** End Of Season (EOS).

SIF-GPP relationship

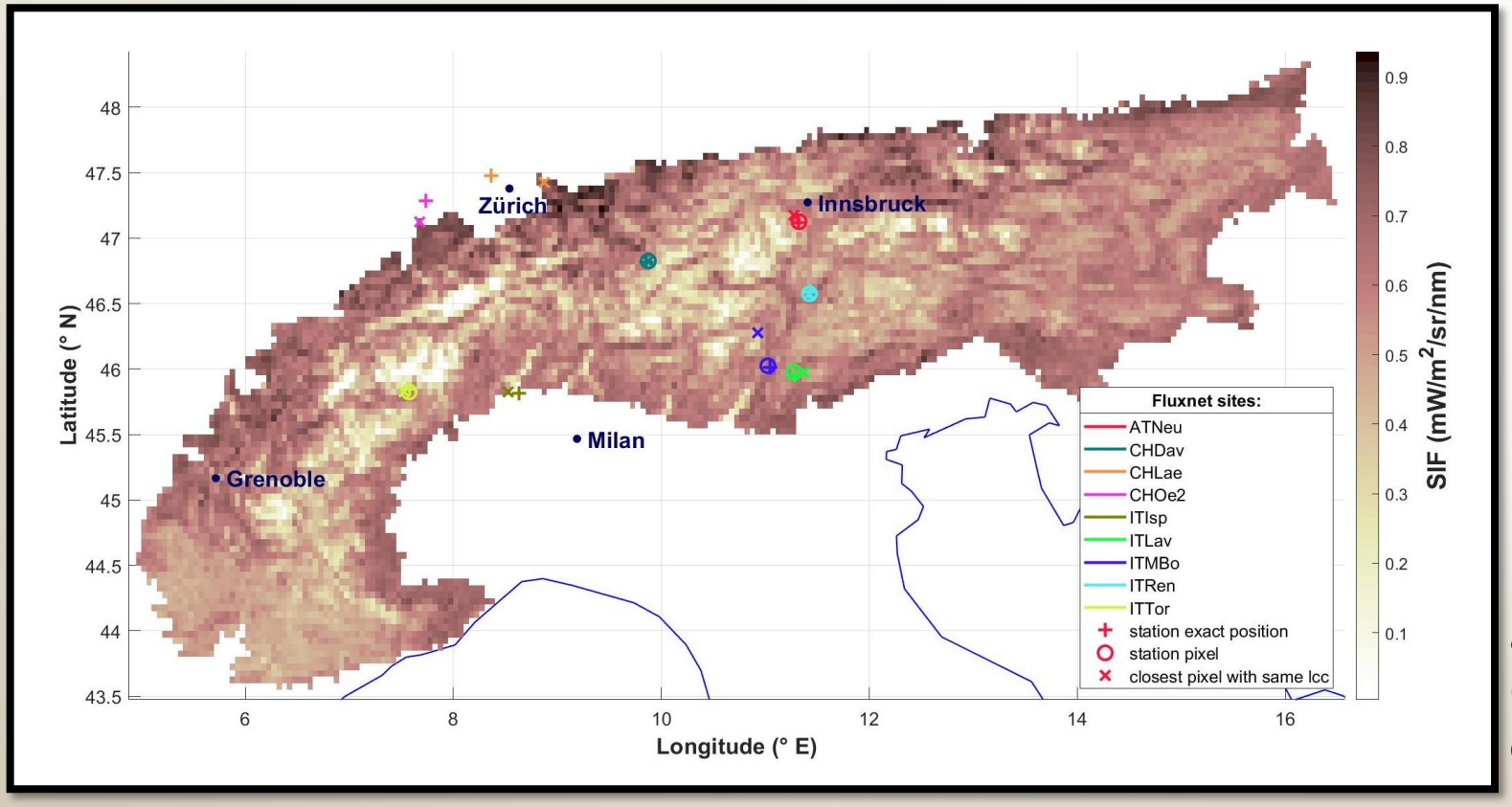

- Fluxnet sites (Alps)
- Same LC to SIF pixels
- Elevation + Location potentially different

Fig. 9 – EC-flux towers sites. Locations of Fluxnet sites and approximated position within GOME-2 downscaled SIF 0.05° x 0.05° pixel grid.

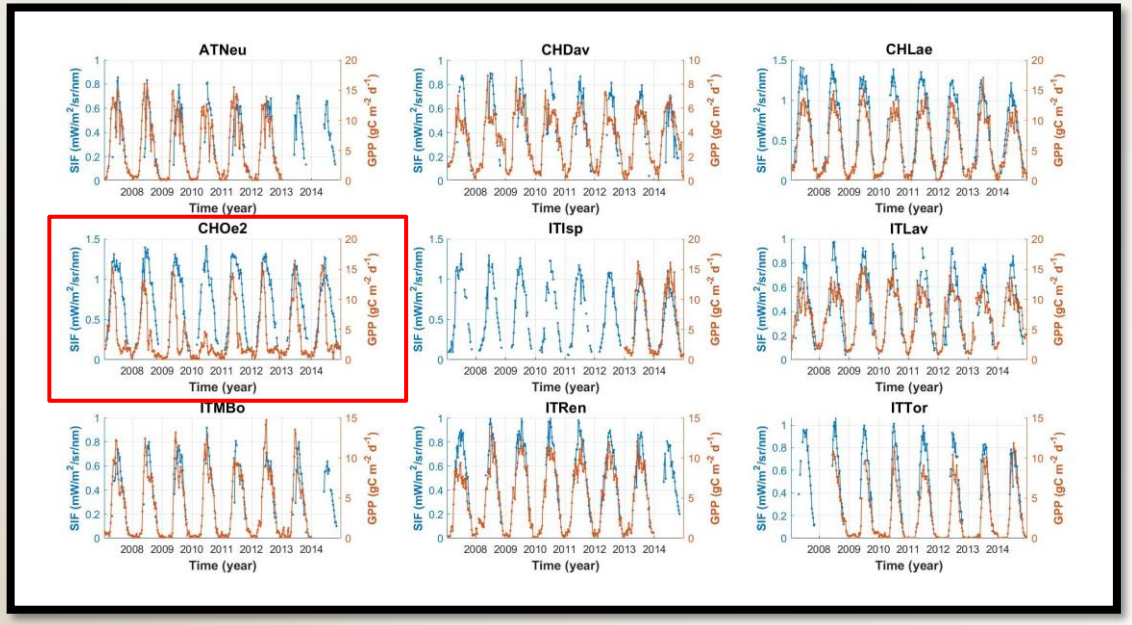

Fig. 10 – SIF vs GPP over time.
Temporal GPP variation from Fluxnet sites and downscaled GOME-2 SIF from pixels close to the sites and with the same dominant land cover class; blue = SIF; orange = GPP.

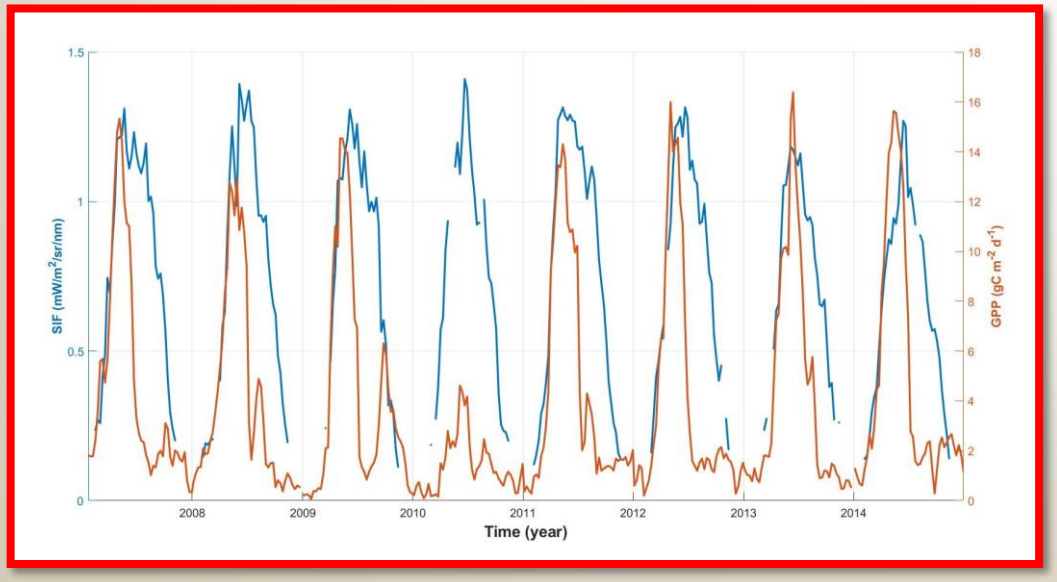

Fig. 11 – SIF vs GPP at the CH-Oe2 site.
Temporal GPP variation at CH-Oe2 site, and downscaled GOME-2 SIF from the closest pixel within the Alps with dominant land cover class "temporary crops".

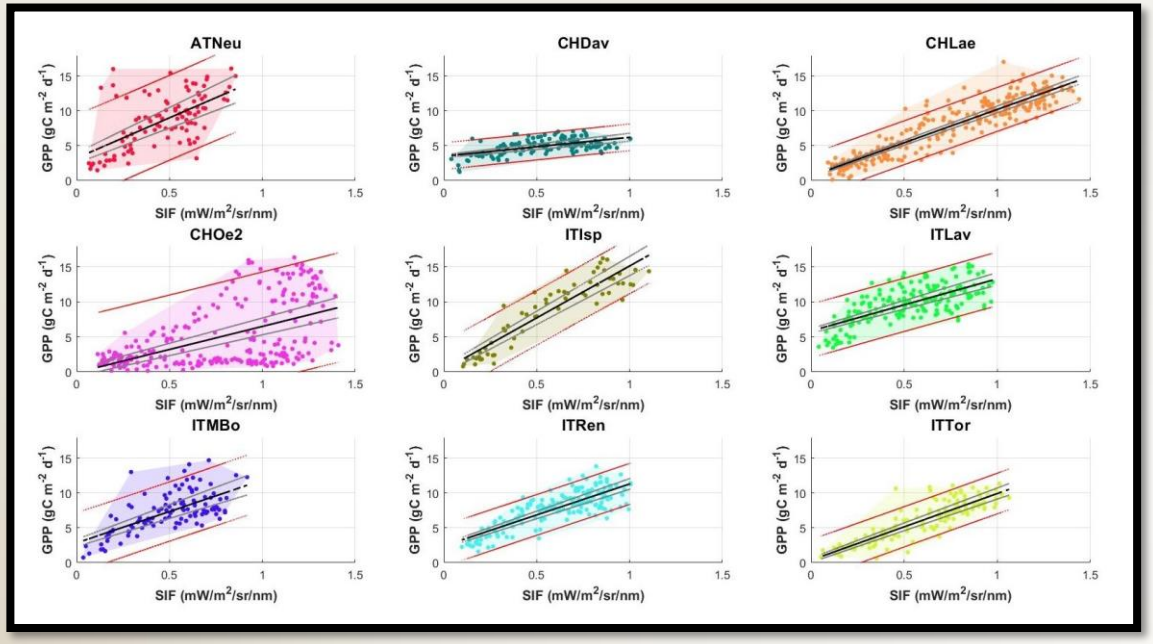

Fig. 12 – SIF-GPP relationship.

SIF-GPP relationship at every flux tower site.

Dots: data points; semi-transparent area: data range; black line: trend line after linear regression model; grey lines: standard error of line coefficients; red lines: 95 % prediction interval.

Table 1 – Z-test for the SIF-GPP relationship.

Z-test for the slope coefficients for each combination of two sites. Significant differences at the 95 % confidence interval are marked.

Site	AT-Neu	CH-Dav	CH-Lae	CH-Oe2	IT-Isp	IT-Lav	IT-MBo	IT-Ren	IT-Tor
AT-Neu	--	5.85	1.34	3.10	1.93	2.62	1.45	1.73	1.29
CH-Dav	5.85	--	15.37	5.24	13.26	6.98	6.16	10.50	11.33
CH-Lae	1.34	15.37	--	4.28	5.99	3.38	0.55	1.25	0.00
CH-Oe2	3.10	5.24	4.28	--	7.78	0.99	2.11	2.91	3.69
IT-Isp	1.93	13.26	5.99	7.78	--	7.27	4.56	6.18	5.43
IT-Lav	2.62	6.98	3.38	0.99	7.27	--	1.42	1.98	2.83
IT-MBo	1.45	6.16	0.55	2.11	4.56	1.42	--	0.12	0.51
IT-Ren	1.73	10.50	1.25	2.91	6.18	1.98	0.12	--	0.99
IT-Tor	1.29	11.33	0.00	3.69	5.43	2.83	0.51	0.99	--

Limitations

- Spatial resolution!
- Data mismatch
  - SIF *vs* environmental parameters
  - Remote sensing *vs* ground measurements
- Year-to-year variability
- Biased LCC representation

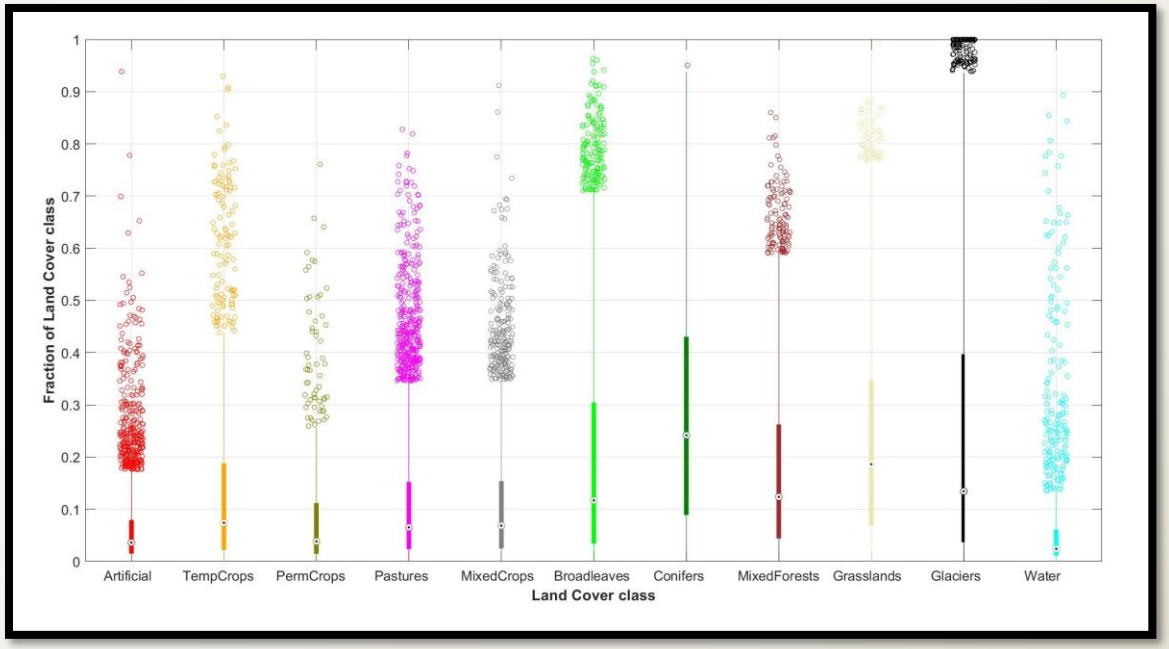

Fig. 13 – LCC Boxplot.
Descriptive statistics for the relative contribution of Land Cover Classes within GOME-2 downscaled 0.05° x 0.05° pixels over the total study area (number of pixels N = 8,514 x 11).

Conclusions

- First study on SIF over the Alps
- General trends and patterns could be analysed, but no fine scale dynamics
- Alps:
  - SIF likely correlated to land cover and elevation
  - SIF-GPP relationship biome-specific, with possibly additional site-specificity

Acknowledgements

- Dr. Karolina Sakowska
- MSc Sebastian Gstir
- Prof. Dr. Erich Tasser
- Dr. Lukas Hörtnagl
- FLUXNET community

Literature

- **Gomarasca, U., Satellite Based Sun-Induced Chlorophyll Fluorescence in the Greater Alpine Space: Spatial Patterns and Relationship to Gross Primary Productivity (2020). Print.**
- G. Duveiller *et al.*, 'A spatially downscaled sun-induced fluorescence global product for enhanced monitoring of vegetation productivity', *Earth Syst. Sci. Data Discuss.*, pp. 1–24, Aug. 2019, doi: 10.5194/essd-2019-121.
- A. Gonsamo, J. M. Chen, and P. D'Odorico, 'Deriving land surface phenology indicators from CO2 eddy covariance measurements', *Ecol. Indic.*, vol. 29, pp. 203–207, 2013, doi: 10.1016/j.ecolind.2012.12.026.

Land Cover Classes (LCC)

Land Cover Class (LCC)	Corine Land Cover (LABEL3)	CLC code
Artificial	Continuous urban fabric	111
	Discontinuous urban fabric	112
	Industrial or commercial units	121
	Road and rail networks and associated land	122
	Port areas	123
	Airports	124
	Mineral extraction sites	131
	Dump sites	132
	Construction sites	133
	Green urban areas	141
	Sport and leisure facilities	142
Temporary crops (TempCrops)	Non-irrigated arable land	211
	Permanently irrigated land	212
	Rice fields	213
Permanent crops (PermCrops)	Vineyards	221
	Fruit trees and berry plantations	222
	Olive groves	223
Pastures	Pastures	231
Mixed crops (MixedCrops)	Annual crops associated with permanent crops	241
	Complex cultivation patterns	242
	Land principally occupied by agriculture	243
	Agro-forestry areas	244
Broadleaves	Broad-leaved forest	311
Conifers	Coniferous forest	312
Mixed forests	Mixed forest	313
Grasslands	Natural grasslands	321
	Moors and heathland	322
	Sclerophyllous vegetation	323
	Transitional woodland-shrub	324
Glaciers	Beaches	331
	Bare rocks	332
	Sparsely vegetated areas	333
	Burnt areas	334
	Glaciers and perpetual snow	335
Water	Inland marshes	411
	Peat bogs	412
	Salt marshes	421
	Salines	422
	Intertidal flats	423
	Water courses	511
	Water bodies	512
	Coastal lagoons	521
	Estuaries	522
	Sea and ocean	523

Table A – Land Cover Classes.
Eleven Land Cover classes defined in this study, and corresponding land cover types with codes from the Corine Land Cover coding system.

SIF-GPP linear regression

Table B – Statistics for the SIF-GPP linear regression model.
Linear regression model statistics for the EC-flux tower sites analysed.

Site	Slope	SEslope	Intercept	SEintercept	df	R2
AT-Neu	11.56	1.47	3.24	0.74	102	0.38
CH-Dav	2.71	0.36	3.51	0.21	132	0.30
CH-Lae	9.57	0.26	0.65	0.23	245	0.85
CH-Oe2	6.59	0.65	-0.07	0.56	257	0.29
IT-Isp	14.83	0.84	0.32	0.54	60	0.84
IT-Lav	7.44	0.57	5.87	0.33	178	0.49
IT-Mbo	9.02	0.96	2.84	0.52	113	0.44
IT-Ren	8.90	0.47	2.41	0.31	172	0.68
IT-Tor	9.57	0.49	0.37	0.31	130	0.75